ANNALS of Clinical and Translational Neurology
Open Access
ANA American Neurological Association since 1875

RESEARCH PAPER

Multimodal MRI-based imputation of the Aβ+ in early mild cognitive impairment

Duygu Tosun[1,a], Sarang Joshi[2], Michael W. Weiner[1] & for the Alzheimer's Disease Neuroimaging Initiative[a]

[1]Department of Radiology and Biomedical Imaging, University of California – San Francisco, San Francisco, California
[2]Scientific Computing and Imaging Institute, University of Utah, Salt Lake City, Utah, 84112

Correspondence
Duygu Tosun, 4150 Clement St., SFVA Medical Center, Bld 13, 114M, San Francisco, CA 94121. Tel: 415-221-4810 (ext. 4800); Fax: 415-386-3849; E-mail: duygu.tosun@ucsf.edu

Funding Information
This study is funded by the National Institutes of Health (NIH) (Grant P41 RR023953). Data collection and sharing for this project were funded by the Alzheimer's Disease Neuroimaging Initiative (ADNI) (National Institutes of Health Grant U01 AG024904). ADNI is funded by the National Institute on Aging, the National Institute of Biomedical Imaging and Bioengineering, and through generous contributions from the following: Alzheimer's Association; Alzheimer's Drug Discovery Foundation; BioClinica, Inc.; Biogen Idec Inc.; Bristol-Myers Squibb Company; Eisai Inc.; Elan Pharmaceuticals, Inc.; Eli Lilly and Company; F. Hoffmann-La Roche Ltd and its affiliated company Genentech, Inc.; GE Healthcare; Innogenetics, N.V.; IXICO Ltd.; Janssen Alzheimer Immunotherapy Research & Development, LLC.; Johnson & Johnson Pharmaceutical Research & Development LLC.; Medpace, Inc.; Merck & Co., Inc.; Meso Scale Diagnostics, LLC.; NeuroRx Research; Novartis Pharmaceuticals Corporation; Pfizer Inc.; Piramal Imaging; Servier; Synarc Inc.; and Takeda Pharmaceutical Company. The Canadian Institutes of Health Research is providing funds to support ADNI clinical sites in Canada. Private sector contributions are facilitated by the Foundation for the National Institutes of Health (www.fnih.org). The grantee organization is the Northern California Institute for Research and Education, and the study is coordinated by the Alzheimer's Disease Cooperative Study at the University of California, San Diego. ADNI data are disseminated by the Laboratory for

Abstract

Objective: The primary goal of this study was to identify brain atrophy from structural MRI (magnetic resonance imaging) and cerebral blood flow (CBF) patterns from arterial spin labeling perfusion MRI that are best predictors of the Aβ-burden, measured as composite ^{18}F-AV45-PET (positron emission tomography) uptake, in individuals with early mild cognitive impairment (MCI). Furthermore, another objective was to assess the relative importance of imaging modalities in classification of Aβ+/Aβ− early MCI. **Methods**: Sixty-seven Alzheimer's Disease Neuroimaging Initiative (ADNI)-GO/2 participants with early MCI were included. Voxel-wise anatomical shape variation measures were computed by estimating the initial diffeomorphic mapping momenta from an unbiased control template. CBF measures normalized to average motor cortex CBF were mapped onto the template space. Using partial least squares regression, we identified the structural and CBF signatures of Aβ after accounting for normal cofounding effects of age, gender, and education. **Results**: ^{18}F-AV45-positive early MCIs could be identified with 83% classification accuracy, 87% positive predictive value, and 84% negative predictive value by multidisciplinary classifiers combining demographics data, ApoE ε4-genotype, and a multimodal MRI-based Aβ score. **Interpretation**: Multimodal MRI can be used to predict the amyloid status of early-MCI individuals. MRI is a very attractive candidate for the identification of inexpensive and noninvasive surrogate biomarkers of Aβ deposition. Our approach is expected to have value for the identification of individuals likely to be Aβ+ in circumstances where cost or logistical problems prevent Aβ detection using cerebrospinal fluid analysis or Aβ-PET. This can also be used in clinical settings and clinical trials, aiding subject recruitment and evaluation of treatment efficacy. Imputation of the Aβ-positivity status could also complement Aβ-PET by identifying individuals who would benefit the most from this assessment.

Neuro Imaging at the University of California, Los Angeles. This research was also supported by NIH grants P30 AG010129 and K01 AG030514.

Received: 6 November 2013; Revised: 16 January 2014; Accepted: 17 January 2014

Annals of Clinical and Translational Neurology **2014; 1(3): 160–170**

doi: 10.1002/acn3.40

[a]Data used in preparation of this article were obtained from the Alzheimer's Disease Neuroimaging Initiative (ADNI) database (adni.loni.ucla.edu). As such, the investigators within the ADNI contributed to the design and implementation of ADNI and/or provided data but did not participate in analysis or writing of this report. A complete listing of ADNI investigators can be found at: http://adni.loni.ucla.edu/wp-content/uploads/how_to_apply/ADNI_Acknowledgement_List.pdf.

Introduction

Amyloid-β (Aβ) peptides form cortical plaques, a major feature of Alzheimer's disease (AD) neuropathology.[1] Approximately 30–50% of brains from the individuals with latent or prodromal AD over age 60 harbor Aβ-pathology in a similar pattern to that seen in AD.[1] In the Alzheimer's Disease Neuroimaging Initiative (ADNI) study 46% of patients with early mild cognitive impairment (MCI) were Aβ-positive, suggesting that these subjects had prodromal AD, while 54% did not have significant brain Aβ accumulation. These findings, together with many other reports[2,3] indicate that clinical assessment alone has limited utility to detect early AD pathology in many individuals. Whether these individuals will later develop cognitive decline and dementia due to AD remains unknown; however, evidence of brain Aβ accumulation increases the risk for progression from clinical dementia rating (CDR) 0 to CDR 0.5 status by fivefold, and conversion from MCI to AD by threefold.[4] Therefore, earlier, more accurate, biomarker-based detection of AD-related Aβ pathology is crucial and could potentially offer a greater opportunity for initiation of disease-modifying therapies prior to the advanced stages of AD.

Brain Aβ deposition can be detected by molecular imaging techniques such as positron emission tomography (PET) using an Aβ-specific radioligand, or through measurement of cerebrospinal fluid (CSF) $A\beta_{1\text{-}42}$ concentration. Both of these measures show high correlations with postmortem measures of fibrillar Aβ.[5–7] Lumbar puncture, required for CSF sample collection, carries a 4% risk of a clinically significant adverse event (e.g., post-lumbar puncture headache, moderate atypical headache, moderate low back pain, vasovagal episode)[8] and is, therefore, unattractive as a population screening tool, particularly in early-stage individuals. Neuroimaging has the advantage of being less invasive and PET tracers have been changing the field by enabling in vivo Aβ plaque detection. However, PET is relatively expensive with limited availability and contributes to the patient's overall long-term cumulative radiation exposure, which is associated with an increased risk of cancer.[9]

There is an emerging literature investigating Aβ-related brain changes using structural MRI (magnetic resonance imaging) describing an association between Aβ burden (e.g., low CSF $A\beta_{1\text{-}42}$ or high Aβ-PET binding) and atrophy, especially of the parietal and posterior cingulate regions, extending into the precuneus and medial temporal regions including hippocampus, amygdala, and entorhinal cortex.[10–16] Although not as substantial as the structural studies, arterial spin labeling (ASL) MRI studies also show Aβ-related cerebral blood flow (CBF) changes including reduced CBF in the cingulate, supramarginal gyrus, thalamus, and midbrain, as well as increased CBF in the medial and inferior frontal, precuneus, and inferior parietal regions.[17–19] These findings suggest that Aβ accumulation is associated with structural and CBF changes, both of which can be detected with MRI.

The primary goal of this study was to develop a method to predict which subjects with early MCI have Aβ deposition, by using MRI-detected changes of brain structure and CBF.

The study cohort consisted of 67 individuals with early MCI between the ages of 60 and 85 years and 33 Aβ-negative cognitively normal (CN) elderly individuals, to model the normal confounding effects of age, gender, and education, all recruited by ADNI. Global Aβ burden, determined by Aβ PET using ^{18}F-AV45 radioligand (florbetapir), served as outcome variable in primary hypotheses testing. The predictors included high-dimensional measures of anatomical shape variations from structural MRI and regional CBF from ASL-MRI, as well as demographics and Apolipoprotein E (ApoE) genotype. Our central hypothesis was that even the earliest Aβ-related structural and CBF changes could be detected in vivo using clinically viable metrics to construct a robust mathematical Aβ prediction model. This will help to develop clinically viable early surrogate biomarkers of AD pathology in prodromal individuals. This will have a broad use in early diagnosis, facilitating initiation of prevention strategies in those at risk, and boost the power of anti-Aβ immunotherapy trials by selecting those at greatest risk of AD. As a secondary goal, we assessed the relative importance of imaging modalities in classification of ^{18}F-AV45-positive versus ^{18}F-AV45-negative early-MCI individuals.

Methods

Participants

Data used in the preparation of this article were obtained from the ADNI database (adni.loni.ucla.edu). The ADNI was launched in 2003 by the National Institute on Aging, the National Institute of Biomedical Imaging and Bioengineering, the Food and Drug Administration, private pharmaceutical companies and non-profit organizations, as a $60 million, 5-year public private partnership. The primary goal of ADNI has been to test whether serial MRI, PET, other biological markers, and clinical and neuropsychological assessment can be combined to measure the progression of MCI and early AD. Determination of sensitive and specific markers of very early AD progression is intended to aid researchers and clinicians to develop new treatments and monitor their effectiveness, as well as to lessen the time and cost of clinical trials.

The Principal Investigator of this initiative is Michael W. Weiner, MD, VA Medical Center and University of California – San Francisco. ADNI is the result of efforts of many co investigators from a broad range of academic institutions and private corporations, and subjects have been recruited from over 50 sites across the U.S. and Canada. The initial goal of ADNI was to recruit 800 subjects but ADNI has been followed by ADNI-GO and ADNI-2. To date, these three protocols have recruited over 1500 adults, ages 55–90, to participate in the research, consisting of CN older individuals, people with early or late MCI, and people with early AD. The follow-up duration of each group is specified in the protocols for ADNI-1, ADNI-2 and ADNI-GO. Subjects originally recruited for ADNI-1 and ADNI-GO had the option to be followed in ADNI-2. For up-to-date information, see www.adni-info.org.

Data for this study were limited to baseline scans from ADNI-GO/2 participants in the ASL-MRI substudy as of June 2013. This cohort included 33 CN elderly individuals (CN) and 67 early-MCI subjects, representative of the broader ADNI-GO/2 CN and early-MCI participants (cf Tables S1–S2). Full inclusion and exclusion criteria for ADNI are described at www.adni-info.org. In brief, CN subjects had mini-mental state examination (MMSE) scores between 24 and 30, a CDR of 0, no evidence of depression, and no memory complaints. Individuals with MCI were classified essentially in the manner described by Petersen,[20] but were then further divided into an "early" and "late" group based on performance on the Wechsler Memory Scale–Revised Logical Memory II (WMS-LM). The early-MCI group was defined based on scores between the cutoff of CN and that of the late-MCI group.

Baseline MRIs of CN subjects were used to model the normal confounding effects of age, gender, and education on anatomical shape variation and CBF measures. Previous studies reported that the cumulative and regional Aβ burden in CN subjects correlate with regional brain atrophy and CBF changes.[10,17,21] Furthermore, CN subjects at genetic risk for AD by virtue of the ApoE ε4-allele demonstrated regional brain atrophy and CBF differences relative to ε4-noncarriers.[22,23] Therefore, we included only the ApoE ε4-noncarrier CN subjects who were identified as Aβ-negative using ^{18}F-AV45-PET. Furthermore, ApoE ε2-allele carrier CN and early-MCI subjects were excluded due to sample size limitations. Study group demographics are summarized in Table 1.

Table 1. Demographic information of subject groups.

	Cognitively healthy elderly	Early MCI	*P*-value
Number of subjects	33	67	–
Age	72.80 ± 6.04	69.76 ± 6.61	0.025
Gender (F/M)	19/14	22/45	0.040
Education	16.70 ± 2.30	16.57 ± 2.66	0.788
ApoE ε4 genotype (ε3/ε3, ε3/ε4, ε4/ε4)	33, 0, 0	41, 23, 3	<0.0001
MMSE	29.24 ± 1.06	28.79 ± 1.21	0.061
CDR-SB	0.02 ± 0.09	1.23 ± 0.81	<0.0001
ADAS-Cog	6.42 ± 3.56	7.65 ± 3.35	0.094
^{18}F-AV45-PET SUVR	1.00 ± 0.05	1.16 ± 0.18	<0.0001
^{18}F-AV45-positive (%)	0%	50%	<0.0001

^{18}F-AV45-PET

^{18}F-AV45-PET scans were acquired 50–70 min after injection of 10 mCi of tracer. Images underwent a rigorous quality control protocol and were processed to produce final images with standard orientation, voxel size, and 8 mm resolution by the ADNI-PET Core.[24] Briefly, scans were analyzed in native space using the subjects' structural MRIs acquired close to the time of the ^{18}F-AV45-PET scans. Structural MRIs were segmented into cortical regions using FreeSurfer version 4.5.0 (surfer.nmr.mgh.harvard.edu/). These cortical regions of interest (ROIs) were used to extract ^{18}F-AV45-PET uptake from gray matter (GM) in lateral and medial frontal, anterior, and posterior cingulate, lateral parietal, and lateral temporal cortex. Values were normalized to florbetapir-PET uptake in the whole cerebellum. The averaged cortical uptake in this composite ROI was used as the index of florbetapir-PET uptake, that is, standard uptake value ratio (SUVR), in each subject. Furthermore, subjects were characterized as ^{18}F-AV45-positive or ^{18}F-AV45-negative based on a threshold value of 1.11 for the ^{18}F-AV45-SUVR.[25]

Multimodality MRI acquisition

Both high-resolution structural MRI and ASL-MRI were acquired at ADNI-GO/2 sites equipped with 3T Siemens MRI scanners. Two structural MRIs were acquired using a 3D magnetization prepared rapid gradient echo (MPRAGE) T1-weighted sequence with the following parameters: TR/TE/TI = 2300/2.98/900 msec, 176 sagittal slices, within plane field-of-view (FOV) = 256 × 240 mm^2, voxel size = 1.1 × 1.1 × 1.2 mm^3, flip angle = 9°, bandwidth = 240 Hz/pix. A designated center selected the MPRAGE image with higher quality and corrected for system-specific image artifacts such as geometry distortion, B1 nonuniformity, and intensity inhomogeneities.[26] ASL-MRIs were acquired using the Siemens product proximal inversion with control for off-resonance effects sequence, which is a pulsed ASL sequence using the Q2TIPs technique for defining the spin bolus. The acquisition parameters were: TR/TE = 3400/12 msec, TI1/TI2 = 700/1900 msec, FOV = 256 mm, 24 sequential 4-mm thick slices with a 25% gap between the adjacent slices, partial Fourier factor = 6/8, bandwidth = 2368 Hz/pix, and imaging matrix = 64 × 64.

Anatomical shape variations

Skull, scalp, and extracranial tissue were removed from each structural MRI using the automated Brain Surface Extraction software,[27] followed by manual refinement if required. To avoid bias toward a particular subject's geometry in analysis of anatomical shape variations, we used the data from CNs to create a study-specific unbiased large deformation brain image template (ULD-template) by applying a framework of large deformation diffeomorphic metric mapping (LDDMM) as described in full elsewhere.[28] ULD-template generation incorporated an unbiased approach where all brain images were first simultaneously affine transformed to adjust for global variations in brain positioning and scale, and then simultaneously deformed. Structural MRI of each early-MCI subject was first affine aligned and then nonlinearly warped to this ULD-template using the LDDMM framework. The LDDMM was modeled as an evolution in time, with an associated smooth velocity vector field controlling this evolution. A scalar initial momentum map parameterized the entire geodesic with which the optimal trajectory emanated from the ULD-template to reach a subject brain image on a Riemannian manifold of diffeomorphism.[28] These momentum maps uniquely encoded the anatomical shape variations of individual brains relative to the ULD-template.

Cerebral blood flow

ASL-MRI processing was performed to obtain partial volume-corrected maps of CBF, as previously described.[29–33] Individual ASL-MRI frames were coregistered using rigid body registration to reduce movement artifacts. Geometric distortion correction on ASL-MRI with respect to the affine-aligned T2-weighted MRI was estimated using a variation image-based approach for correction of susceptibility artifacts.[34] Motion and distortion corrected images were normalized to the ASL reference scan signal (the first volume of the ASL acquisitions), without background suppression, to account for B1-field variations. The dynamic ASL data were fitted voxel-by-voxel to a dual compartment perfusion model, which takes into account variable transit times, bolus durations, distributed concentrations of capillary water and restricted brain-blood barrier permeability.[35] This model yielded a parametric map for CBF. The ASL reference scan signal without background suppression was rigidly coregistered, first to T2-weighted and then to MPRAGE-MRI, to map the parametric CBF measures to the structural-imaging space, where anatomical tissue compartments were defined by an adaptive fuzzy c-means algorithm.[36] Variations of CBF due to partially volumed GM voxels were accounted for by voxel-wise analysis of covariance, in which the tissue compartment estimates were entered as regressors. To account for global variations in CBF between and within individuals, CBF maps were intensity normalized by average CBF in the motor cortex, which is spared in AD. The resultant CBF maps were resampled to the ULD-template

image space via the corresponding LDDMM vector fields, estimated for the corresponding structural MRI.

Covariates

We used a general linear model based detrending method to control for any normal confounding effects of age, gender, and education, based on ^{18}F-AV45-negative and ApoE ε3/ε3 CN subjects. Adjusted imaging measures of anatomical shape variation and CBF were used for further data analyses.

Neuroimaging correlates of Aβ burden

MR imaging provides high-throughput data for discovery of surrogate biomarkers for Aβ pathology, but the high-dimensional data based on a relatively small number of participants inherently comes with significant codependencies and contain a large number of association patterns, most of which are erroneous or redundant. Our goal was to identify which of these are significant associations, with high predictive power. Partial least squares (PLS) regression[37] has the ability to handle high-dimension, low sample size, multicollinear data, while searching for modes that explain the maximum covariance between the explanatory and response spaces. We used PLS regression with the neuroimaging measures (i.e., anatomical shape variation and CBF) from each and every imaging voxel as predictors to assess the patterns of neuroimaging-Aβ associations. In joint analysis of anatomical shape variation and CBF measures, we first normalized each imaging data to have unit variance and then combined the data to form a product space defined by their convex combination with a relative weighting coefficient of $0 \leq \lambda \leq 1$, that is, $\lambda = 0$ for pure CBF correlates of Aβ and $\lambda = 1$ for pure anatomical shape variation correlates of Aβ. For a given λ, the statistical significance of the neuroimaging-Aβ associations inferred by PLS regression was assessed using the projected data and non-parametric permutation testing. Furthermore, a λ-dependent neuroimaging-based Aβ score was calculated by projecting each individual's neuroimaging data onto the latent variable (LV) inferred by the corresponding PLS regression.

Classification of Aβ+ early-MCI individuals

To create a mathematical function that best combines the neuroimaging-based Aβ score, demographics (i.e., age, gender, and education), and ApoE genotype to give a binary prediction of Aβ+ in early-MCI individuals, we based our classification model to a logistic regression with least absolute shrinkage and selection operator (LASSO). The neuroimaging-based Aβ score, age, gender, education, and ApoE genotype were the independent predictor variables. The dependent outcome variable was the Aβ+/− dichotomization, based on ^{18}F-AV45-PET scans and established standardized ^{18}F-AV45 uptake threshold.[25] For 10-fold cross-validation of the classifier performance, the data were divided into 10 subsets of cases that had similar size and Aβ+/− distributions. Each subset was left out once, while the other nine was applied to construct a neuroimaging-based Aβ score and a classifier subsequently validated for the unseen cases in the left-out subset. Classifier performance assessment was based on classification accuracy (CA), positive predictive value (PPV), and negative predictive value (NPV). Performance of the best performing classifier with nonimaging factors was referenced to test the added value of neuroimaging in classification of Aβ+/Aβ− early MCI. Finally, to assess the relative importance of structural and ASL imaging data, we constructed the neuroimaging-based Aβ score and classifier for various λ values in the range (0, 1) with 0.05 increments.

Results

Demographic characteristics

Demographic characteristics of the subjects are summarized in Table 1. On average, early MCIs were significantly younger than CNs ($t = 2.29$, $P = 0.02$), although still in the same age range. Early-MCI group had disproportionately higher male subjects compared with CN group ($\chi^2 = 4.23$, $P = 0.04$). Consistent with the ADNI recruitment criteria and our study design, early-MCI and CN groups differed in the clinical measure of CDR-SB, ^{18}F-AV45-SUVR (two-sample t-tests; $P < 0.0001$), ^{18}F-AV45-positive/negative ratio, and ApoE ε4-allele frequency (chi-squared contingency table test; $P < 0.0001$).

Neuroimaging signatures of brain amyloidosis

Figure 1A shows the spatial signature of the LV inferred by PLS regression for $\lambda = 1$, that is, anatomical shape variation signature of brain Aβ-burden in early MCI. Dark red/blue and white colors indicate greater contribution of the local anatomical shape variations to the LV, therefore to the structural-Aβ association. Increased ^{18}F-AV45-SUVR was associated with anatomical shape variations largely in the frontoparietal cortical regions including inferior parietal, precuneus, supramarginal, postcentral, middle frontal, and to a lesser extent in the temporal lobe regions including superior temporal, entorhinal, hippocampus, and subcortical regions including amygdala, nucleus accumbens, and caudate ($r = 0.93$; $P < 0.0001$).

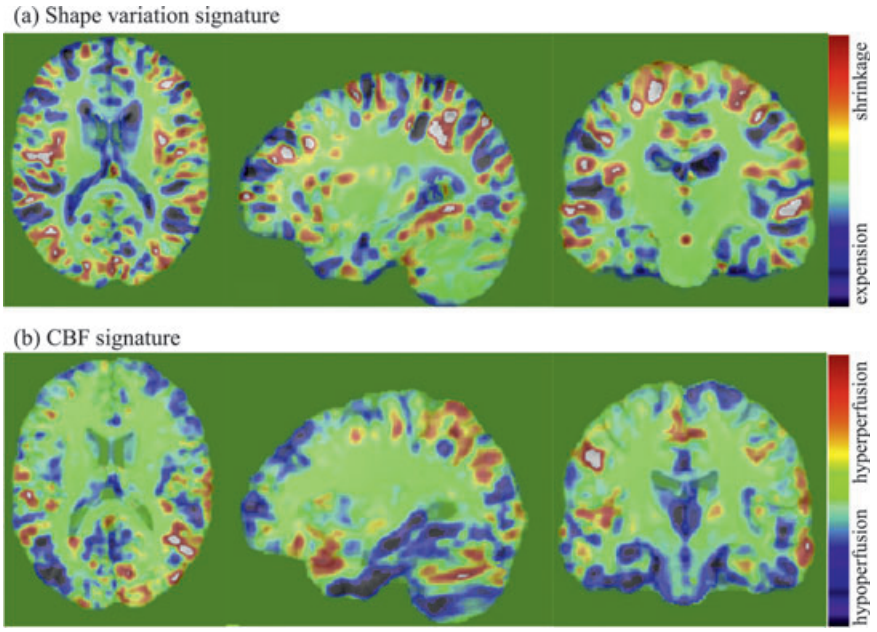

Figure 1. Neuroimaging signatures of brain amyloidosis in early MCI.

The spatial signature of the LV inferred by PLS regression for $\lambda = 0$, that is, CBF signature of brain Aβ-burden in early MCI, is shown in Figure 1B. Hypoperfusion regions are colored in shades of blue and hyperperfusion regions are colored in shades of red. Increased ^{18}F-AV45-SUVR was associated with hypoperfusion primarily in the medial temporal regions, including hippocampus, entorhinal, parahippocampus, fusiform, temporal pole, amygdala, as well as with hyperperfusion largely localized in the inferior parietal lobule but also including inferior frontal, postcentral, and precuneus regions ($r = 0.77$; $P < 0.0001$).

Aβ+ predictive power of the neuroimaging-based Aβ scores alone and in combination with other nonimaging variables

Estimated performances of the LASSO penalized logistic regression classifiers with nonimaging variables (i.e., age, gender, years of education, and ApoE-ε4 genotype) alone and jointly with neuroimaging-based Aβ scores are reported in Table 2. All classifiers considered in this study performed significantly better than chance ($P < 0.01$). ApoE ε4-genotype jointly with demographics data classified ^{18}F-AV45-positive early MCIs with a 69% CA, 73% PPV, and 70% NPV. Both pure structural- and pure ASL-MRI-based Aβ scores outperformed the ApoE ε4-genotype ($P < 0.01$) and reached higher CAs (79% and 75%, respectively), higher PPVs (81% and 76%, respectively), and higher NPVs (80% and 78%, respectively). A multidisciplinary classifier combining demographics, ApoE ε4-genotype, and neuroimaging-based Aβ scores reached 80–83% CA, 82–85% PPV, and 82–83% NPV in identifying ^{18}F-AV45-positive early MCIs.

Table 2. Estimated performances of the LASSO penalized logistic regression classifiers in predicting ^{18}F-AV45-positivity in early MCI.

Predictors	CA	PPV	NPV
Demographics (age, gender, years of education)	0.65 ± 0.03	0.67 ± 0.03	0.66 ± 0.04
Demographics and ApoE ε4 genotype	0.69 ± 0.08	0.73 ± 0.09	0.70 ± 0.10
Demographics and sMRI-based Aβ burden score	0.79 ± 0.05	0.81 ± 0.06	0.80 ± 0.07
Demographics and ASL-based Aβ burden score	0.75 ± 0.11	0.76 ± 0.12	0.78 ± 0.10
Demographics and ApoE ε4 genotype and sMRI-based Aβ burden score	0.83 ± 0.03	0.85 ± 0.02	0.83 ± 0.04
Demographics and ApoE ε4 genotype and ASL-based Aβ burden score	0.80 ± 0.06	0.82 ± 0.06	0.82 ± 0.02

Relative importance of imaging modalities in identifying ^{18}F-AV45-positive early MCIs

Performance of the multidisciplinary classifier as a function of λ, relative weighting coefficient for structural MRI and ASL-MRI in the construction of the neuroimaging-

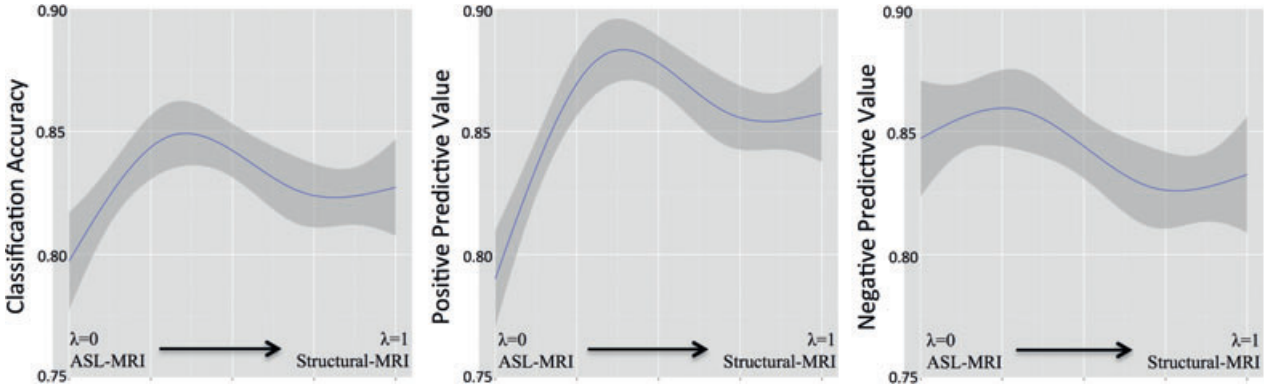

Figure 2. Performance of the multidisciplinary classifier as a function of λ, relative weighting coefficient for structural MRI and ASL-MRI in the construction of the neuroimaging-based Aβ score.

based Aβ score, is plotted in Figure 2. Maximal CA (≥83%), PPV (≥87%), and NPV (≥84%) were achieved with $0.25 \leq \lambda < 0.5$. Added value of multimodality-MRI over unimodality MRI was significant ($P < 0.01$) only in terms of PPV of the final classifier.

Discussion

The major findings of this study were (1) ^{18}F-AV45-positive early-MCI subjects could be identified with a CA ≥ 83%, PPV ≥ 87%, and NPV ≥ 84% by a multidisciplinary classifier combining demographics data, ApoE ε4-genotype, and multimodality MRI-based Aβ score; (2) this maximal ^{18}F-AV45-positivity classifier performance was achieved with a relative weighting coefficient of $0.25 \leq \lambda < 0.5$ for structural MRI and ASL-MRI, implying the dominance of CBF changes in predicting ^{18}F-AV45-positivity in early MCI; and (3) greater cortical ^{18}F-AV45-SUVR in early MCI was associated with patterns of anatomical shape variations predominantly in the fronto-parietal regions, patterns of hypoperfusion in medial temporal cortices, and patterns of hyperperfusion localized to inferior parietal lobule. Taken together these results demonstrate that structural MRI and ASL-MRI can be used to predict the Aβ status of individuals with early MCI.

We previously pursued the use of structural MRI in predicting widespread brain Aβ deposition in individuals with MCI.[38] Although the overall objective of this study is similar to our previous work, the contribution of this study is twofold: First, the primary goal of this study was to develop a method to predict which subjects with early MCI have brain Aβ deposition, by using MRI-detected changes of brain structure and CBF. Expected smaller effect size estimates for both functional and structural brain changes make it challenging to adequately power to construct a robust mathematical Aβ prediction model for early-MCI. Second, to the best of our knowledge, this is the first neuroimaging study showing the value of structural MRI and ASL-MRI as predictors of the likelihood of significant Aβ accumulation, both independently and jointly. According to our findings, the added value of multimodal MRI is incremental yet significant especially in terms of the PPV of the proposed early-MCI Aβ-positivity predictor. We demonstrated that with multimodality MRI, basic demographics, and ApoE genotype data, we could achieve an 83% CA with an 87% PPV and an 85% NPV in identifying ^{18}F-AV45-positive early-MCI. This multimodality/multidisciplinary classification model outperformed other classifiers considered in this study using either nonimaging factors or unimodality neuroimaging data. Such an Aβ-positivity classifier would greatly improve the efficiency of clinical trials targeting the early disease stages by reducing the number of subjects needed to be screened with Aβ-PET scans or lumbar punctures. Specifically, based on the 87% PPV, to enroll 100 ^{18}F-AV45-positive early-MCI participants, screening on structural and CBF variations in addition to age, gender, education, and ApoE genotype can reduce the number needed to screen by 47%, resulting in screening of only 15 additional participants than the targeted number. According to our analyses, the added value of multimodality neuroimaging data to age, gender, education, and ApoE genotype information is a 14% increase in the CA, as well as in PPV and NPV of the final Aβ-positivity prediction model. The 14% difference in PPV and NPV metrics translates to a 20% difference in both the number of subjects needed to screen for recruitment and the number of subjects needed to screen with Aβ-PET scans.

There is an emerging literature investigating Aβ-related brain changes using structural MRI describing an association between Aβ burden (e.g., low CSF $A\beta_{1\text{-}42}$ or high Aβ-PET binding) and atrophy, especially of the parietal and posterior cingulate regions, extending into the precuneus and medial temporal regions including

hippocampus, amygdala, and entorhinal cortex. This parietotemporal dominant pattern of Aβ-atrophy association is even evident at mild stages of cognitive deficits.[10–16,39–41] A surprising finding of this study showed that in early MCI, Aβ-related anatomical shape variations were widespread, and showed a superior–inferior gradient with anatomical shape variations in the parietal and frontal regions exhibiting greater associations with Aβ-burden than temporal and occipital regions. This early-MCI anatomical shape variation signature of brain Aβ is mainly in agreement with the Aβ-accumulation patterns reported for elderly individuals,[2,42] affecting predominantly parietal and frontal brain regions more than temporal and occipital brain regions with a superior–inferior gradient.[2,42] This suggests a localized effect of Aβ pathology on brain structure in early-MCI individuals. In contrast to the structural-Aβ association pattern, the early-MCI CBF signature of brain Aβ involved several AD-related neurodegeneration brain regions, in agreement with many previous reports of altered tempero-parietal CBF in AD continuum.[30,43–52] Our finding of spatial pattern CBF-Aβ association being distributed rather than being localized to Aβ accumulation sites suggests a greater involvement of a memory network including hippocampal complex in Aβ-related CBF changes in early MCI. Future studies examining the temporal dynamics of Aβ accumulation, atrophy, and CBF changes could further our understanding of pathophysiological processes in early disease stages.

The strength of this study is the approach we used to predict the likelihood of significant Aβ accumulation in early MCI. We applied a combination of state-of-the-art, yet clinically feasible, 3T neuroimaging techniques for quantification of voxel-based brain anatomical and CBF changes, and modern multivariate statistical analysis methods that allow simultaneous testing of variations across modalities and brain regions to maximally exploit information and to relate these high-dimensional brain alterations to measure of global brain Aβ accumulation. Although neuroimaging research has made major progress in linking Aβ and AD-related neurodegeneration, the majority of these studies have analyzed each neuroimaging modality in isolation, ignoring relationships between the measures that might carry important predictive information for Aβ-positivity. Moreover, aside from a small number of studies,[38,40,53] most neuroimaging studies and especially those using structural MRI, evaluate variations in the brain region-by-region, ignoring the network connectivity changes that could reflect the pathological footprint of Aβ accumulation.

A potential limitation of this study is that findings from the ADNI may not precisely generalize to general population. In particular, ADNI population represents a clinical trial population and not an epidemiologically selected real life population. Other study limitations include the inherent limitations of the ASL technique, namely that it has low signal-to-noise ratio, and is susceptible to motion artifacts. Finally, our study does not explain the mechanisms behind the detected Aβ-related structural and CBF variations. Furthermore, the neuroimaging signature of brain amyloidosis estimated by the PLS regression approach represents the parsimonious set of neuroimaging variables (i.e., anatomical shape variation or CBF measures from a subset of brain tissue voxels) that cumulatively explain the variance in Aβ burden maximally. These parsimonious set of neuroimaging voxels identified as good predictors of Aβ burden is expected to be smaller than the set of neuroimaging voxels potentially with significant Aβ-association based on conventional voxel-based analysis.

In conclusion, MRI is a very attractive candidate for the identification of inexpensive and noninvasive surrogate biomarkers of Aβ deposition because it is widely available, and routinely assessed in clinical practice. Exploring biomarkers from a range of modalities and/or disciplines already well established in AD research and clinical practice may also provide a less invasive, less expensive, and more practical way to identify individuals with Aβ pathology. Several lines of evidence suggest that clinical measures, genetic risk factors, and peripheral blood protein levels can also reflect the likelihood of having elevated Aβ accumulation and can potentially be useful for assessing the risk for future conversion into AD.[54–59] Together with the work of others, our findings could result in development of multidisciplinary and multimodality biomarkers of brain amyloidosis that are reliable, minimally invasive, simple to perform, and widely available. These may include detailed demographic characteristics such as family history, cognitive performance, and high-throughput biomarker technologies such as genomics and proteomics. Our approach is expected to have value for the identification of individuals likely to be Aβ+ in circumstances where cost or logistical problems prevent Aβ detection using CSF analysis or amyloid PET. This can be used in clinical settings and clinical trials, aiding subject recruitment and evaluation of treatment efficacy. Imputation of the Aβ-positivity status could also complement Aβ-PET by identifying individuals who would benefit the most from this assessment.

Acknowledgments

This study is funded by the National Institutes of Health (NIH) (Grant P41 RR023953). Data collection and sharing for this project were funded by the Alzheimer's Disease Neuroimaging Initiative (ADNI) (National Institutes of Health Grant U01 AG024904). ADNI is funded by the

National Institute on Aging, the National Institute of Biomedical Imaging and Bioengineering, and through generous contributions from the following: Alzheimer's Association; Alzheimer's Drug Discovery Foundation; BioClinica, Inc.; Biogen Idec Inc.; Bristol-Myers Squibb Company; Eisai Inc.; Elan Pharmaceuticals, Inc.; Eli Lilly and Company; F. Hoffmann-La Roche Ltd and its affiliated company Genentech, Inc.; GE Healthcare; Innogenetics, N.V.; IXICO Ltd.; Janssen Alzheimer Immunotherapy Research & Development, LLC.; Johnson & Johnson Pharmaceutical Research & Development LLC.; Medpace, Inc.; Merck & Co., Inc.; Meso Scale Diagnostics, LLC.; NeuroRx Research; Novartis Pharmaceuticals Corporation; Pfizer Inc.; Piramal Imaging; Servier; Synarc Inc.; and Takeda Pharmaceutical Company. The Canadian Institutes of Health Research is providing funds to support ADNI clinical sites in Canada. Private sector contributions are facilitated by the Foundation for the National Institutes of Health (www.fnih.org). The grantee organization is the Northern California Institute for Research and Education, and the study is coordinated by the Alzheimer's Disease Cooperative Study at the University of California, San Diego. ADNI data are disseminated by the Laboratory for Neuro Imaging at the University of California, Los Angeles. This research was also supported by NIH grants P30 AG010129 and K01 AG030514.

Conflict of Interest

None declared.

References

1. Braak H, Thal DR, Ghebremedhin E, Del Tredici K. Stages of the pathologic process in Alzheimer disease: age categories from 1 to 100 years. J Neuropathol Exp Neurol 2011;70:960–969.
2. Pike KE, Savage G, Villemagne VL, et al. β-Amyloid imaging and memory in non-demented individuals: evidence for preclinical Alzheimer's disease. Brain 2007;130:2837–2844.
3. Morris J, Price J. Pathologic correlates of nondemented aging, mild cognitive impairment, and early-stage Alzheimer's disease. J Mol Neurosci 2001;17:101–118.
4. Morris JC, Roe CM, Grant EA, et al. Pittsburgh compound B imaging and prediction of progression from cognitive normality to symptomatic Alzheimer disease. Arch Neurol 2009;66:1469–1475.
5. Clark CM, Pontecorvo MJ, Beach TG, et al. Cerebral PET with florbetapir compared with neuropathology at autopsy for detection of neuritic amyloid-β plaques: a prospective cohort study. Lancet Neurol 2012;11:669–678.
6. Driscoll I, Troncoso J, Rudow G, et al. Correspondence between in vivo 11C-PiB-PET amyloid imaging and postmortem, region-matched assessment of plaques. Acta Neuropathol 2012;124:823–831.
7. Clark CM, Xie S, Chittams J, et al. Cerebrospinal fluid tau and β-amyloid: how well do these biomarkers reflect autopsy-confirmed dementia diagnoses? Arch Neurol 2003;60:1696–1702.
8. Peskind ER, Riekse R, Quinn JF, et al. Safety and acceptability of the research lumbar puncture. Alzheimer Dis Assoc Disord 2005;19:220–225.
9. Griffey RT, Sodickson A. Cumulative radiation exposure and cancer risk estimates in emergency department patients undergoing repeat or multiple CT. AJR Am J Roentgenol 2009;192:887–892.
10. Becker JA, Hedden T, Carmasin J, et al. Amyloid-β associated cortical thinning in clinically normal elderly. Ann Neurol 2011;69:1032–1042.
11. Oh H, Mormino EC, Madison C, et al. β-Amyloid affects frontal and posterior brain networks in normal aging. Neuroimage 2011;54:1887–1895.
12. Whitwell JL, Tosakulwong N, Weigand SD, et al. Does amyloid deposition produce a specific atrophic signature in cognitively normal subjects? Neuroimage Clin 2013;2:249–257.
13. Sabuncu MR, Desikan RS, Sepulcre J, et al. The dynamics of cortical and hippocampal atrophy in Alzheimer disease. Arch Neurol 2011;68:1040–1048.
14. Chetelat G, Villemagne VL, Villain N, et al. Accelerated cortical atrophy in cognitively normal elderly with high beta-amyloid deposition. Neurology 2012;78:477–484.
15. Andrews KA, Modat M, Macdonald KE, et al. Atrophy rates in asymptomatic amyloidosis: implications for Alzheimer prevention trials. PLoS One 2013;8:e58816.
16. Schott JM, Bartlett JW, Fox NC, Barnes J. Increased brain atrophy rates in cognitively normal older adults with low cerebrospinal fluid $Abeta_{1-42}$. Ann Neurol 2010;68:825–834.
17. Sojkova J, Beason-Held L, Zhou Y, et al. Longitudinal cerebral blood flow and amyloid deposition: an emerging pattern? J Nucl Med 2008;49:1465–1471.
18. McLaren D, Schultz AChhatwal J, et al., eds. ApoE e4 and amyloid burden independently increase cerebral blood flow in cognitively normal older adults. Seventh Human Amyloid Imaging; Miami, 2013.
19. Sojkova J, Goh J, Beason-Held L, et al., eds. Increased beta-amyloid deposition is related to regional cerebral blood flow in nondemented older adults. Human Amyloid Imaging 2011 Meeting; Miami, 2011.
20. Petersen RC, Smith GE, Waring SC, et al. Mild cognitive impairment: clinical characterization and outcome. Arch Neurol 1999;56:303–308.
21. Bourgeat P, Chetelat G, Villemagne VL, et al. β-Amyloid burden in the temporal neocortex is related to hippocampal atrophy in elderly subjects without dementia. Neurology 2010;74:121–127.

22. Honea RA, Vidoni E, Harsha A, Burns JM. Impact of APOE on the healthy aging brain: a voxel-based MRI and DTI study. J Alzheimers Dis 2009;18:553–564.
23. Bangen KJ, Restom K, Liu TT, et al. Assessment of Alzheimer's disease risk with functional magnetic resonance imaging: an arterial spin labeling study. J Alzheimers Dis 2012;31(Suppl. 3):S59–S74.
24. Jagust WJ, Bandy D, Chen K, et al. The Alzheimer's disease neuroimaging initiative positron emission tomography core. Alzheimers Dement 2010;6:221–229.
25. Landau SM, Breault C, Joshi AD, et al. Amyloid-beta imaging with Pittsburgh compound B and florbetapir: comparing radiotracers and quantification methods. J Nucl Med 2013;54:70–77.
26. Jack CR, Bernstein MA, Fox NC, et al. The Alzheimer's disease neuroimaging initiative (ADNI): MRI methods. J Magn Reson Imaging 2008;27:685–691.
27. Shattuck DW, Leahy RM. BrainSuite: an automated cortical surface identification tool. Med Image Anal 2002;6:129–142.
28. Jiang T, Navab N, Pluim J, et al., eds. Multivariate statistical analysis of deformation momenta relating anatomical shape to neuropsychological measures. Medical image computing and computer-assisted intervention – MICCAI 2010. Berlin/Heidelberg: Springer, 2010. p. 529–537.
29. Tosun D, Mojabi P, Weiner MW, Schuff N. Joint analysis of structural and perfusion MRI for cognitive assessment and classification of Alzheimer's disease and normal aging. Neuroimage 2010;52:186–197.
30. Johnson NA, Jahng GH, Weiner MW, et al. Pattern of cerebral hypoperfusion in Alzheimer disease and mild cognitive impairment measured with arterial spin-labeling MR imaging: initial experience. Radiology 2005;234:851–859.
31. Hayasaka S, Du A-T, Duarte A, et al. A non-parametric approach for co-analysis of multi-modal brain imaging data: application to Alzheimer's disease. Neuroimage 2006;30:768–779.
32. Du AT, Jahng GH, Hayasaka S, et al. Hypoperfusion in frontotemporal dementia and Alzheimer disease by arterial spin labeling MRI. Neurology 2006;67:1215–1220.
33. Tosun D, Rosen H, Miller BL, et al. MRI patterns of atrophy and hypoperfusion associations across brain regions in frontotemporal dementia. Neuroimage 2012;59:2098–2109.
34. Tao R, Fletcher P, Gerber S, Whitaker R, eds. A variational image-based approach to the correction of susceptibility artifacts in the alignment of diffusion weighted and structural MRI. Inf Process Med Imaging 2009;21:664–675.
35. Li K-L, Zhu X, Hylton N, et al. Four-phase single-capillary stepwise model for kinetics in arterial spin labeling MRI. Magn Reson Med 2005;53:511–518.
36. Pham DL, Prince JL. Adaptive fuzzy segmentation of magnetic resonance images. IEEE Trans Med Imaging 1999;18:737–752.
37. Wold S, Geladi P, Esbensen K, Öhman J. Multi-way principal components-and PLS-analysis. J Chemom 1987;1:41–56.
38. Tosun D, Joshi S, Weiner MW. Neuroimaging predictors of brain amyloidosis in mild cognitive impairment. Ann Neurol 2013;74:188–198.
39. Chetelat G, Villemagne VL, Bourgeat P, et al. Relationship between atrophy and beta-amyloid deposition in Alzheimer disease. Ann Neurol 2010;67:317–324.
40. Tosun D, Schuff N, Mathis CA, et al. Spatial patterns of brain amyloid-β burden and atrophy rate associations in mild cognitive impairment. Brain 2011;134:1077–1088.
41. Tosun D, Schuff N, Truran-Sacrey D, et al. Relations between brain tissue loss, CSF biomarkers, and the ApoE genetic profile: a longitudinal MRI study. Neurobiol Aging 2010;31:1340–1354.
42. Rowe CC, Ng S, Ackermann U, et al. Imaging β-amyloid burden in aging and dementia. Neurology 2007;68:1718–1725.
43. Johnson KA, Mueller ST, Walshe TM, et al. Cerebral perfusion imaging in Alzheimer's disease. Use of single photon emission computed tomography and iofetamine hydrochloride I 123. Arch Neurol 1987;44:165–168.
44. Dougall N, Nobili F, Ebmeier KP. Predicting the accuracy of a diagnosis of Alzheimer's disease with 99mTc HMPAO single photon emission computed tomography. Psychiatry Res 2004;131:157–168.
45. Ishii K, Sasaki M, Yamaji S, et al. Demonstration of decreased posterior cingulate perfusion in mild Alzheimer's disease by means of H215O positron emission tomography. Eur J Nucl Med 1997;24:670–673.
46. Matsuda H, Mizumura S, Nagao T, et al. Automated discrimination between very early Alzheimer disease and controls using an easy Z-score imaging system for multicenter brain perfusion single-photon emission tomography. AJNR Am J Neuroradiol 2007;28:731–736.
47. Alsop DC, Detre JA, Grossman M. Assessment of cerebral blood flow in Alzheimer's disease by spin-labeled magnetic resonance imaging. Ann Neurol 2000;47:93–100.
48. Binnewijzend MA, Kuijer JP, Benedictus MR, et al. Cerebral blood flow measured with 3D pseudocontinuous arterial spin-labeling MR imaging in Alzheimer disease and mild cognitive impairment: a marker for disease severity. Radiology 2013;267:221–230.
49. Dai W, Lopez OL, Carmichael OT, et al. Mild cognitive impairment and Alzheimer disease: patterns of altered cerebral blood flow at MR imaging. Radiology 2009;250:856–866.
50. Alsop DC, Casement M, de Bazelaire C, et al. Hippocampal hyperperfusion in Alzheimer's disease. Neuroimage 2008;42:1267–1274.

51. Alexopoulos P, Sorg C, Forschler A, et al. Perfusion abnormalities in mild cognitive impairment and mild dementia in Alzheimer's disease measured by pulsed arterial spin labeling MRI. Eur Arch Psychiatry Clin Neurosci 2012;262:69–77.
52. Fleisher AS, Podraza KM, Bangen KJ, et al. Cerebral perfusion and oxygenation differences in Alzheimer's disease risk. Neurobiol Aging 2009;30:1737–1748.
53. Oh H, Habeck C, Madison C, Jagust W. Covarying alterations in Abeta deposition, glucose metabolism, and gray matter volume in cognitively normal elderly. Hum Brain Mapp 2014;35:297–308.
54. Mielke M, Wiste H, Wiegand S, eds. Identification of non-invasive screening variables for the prediction of amyloid accumulation in a population-based study of cognitively normal elderly individuals. Alzheimer's Association International Conference. Vancouver, British Columbia, Canada, 14–19 July 2012.
55. Apostolova L, Hwang K, Kohannim O, eds. Predicting brain amyloidosis in MCI using clinical, cognitive, imaging and peripheral blood protein measures. Alzheimer's Association International Conference. Vancouver, British Columbia, Canada, 14–19 July 2012.
56. Perrotin A, Mormino EC, Madison CM, et al. Subjective cognition and amyloid deposition imaging: a Pittsburgh compound B positron emission tomography study in normal elderly individuals. Arch Neurol 2012;69:223–229.
57. Hedden T, Oh H, Younger AP, Patel TA. Meta-analysis of amyloid-cognition relations in cognitively normal older adults. Neurology 2013;80:1341–1348.
58. Amariglio RE, Becker JA, Carmasin J, et al. Subjective cognitive complaints and amyloid burden in cognitively normal older individuals. Neuropsychologia 2012;50:2880–2886.
59. Mosconi L, Rinne JO, Tsui WH, et al. Increased fibrillar amyloid-{beta} burden in normal individuals with a family history of late-onset Alzheimer's. Proc Natl Acad Sci USA 2010;107:5949–5954.

Supporting Information

Additional Supporting Information may be found in the online version of this article:

Table S1. Demographic information of cognitively healthy elderly subjects in full ADNI-GO/2 study versus ASL-MRI substudy.
Table S2. Demographic information of early-MCI subjects in full ADNI-GO/2 study versus ASL-MRI substudy.

